Received August 4, 2021, accepted August 28, 2021, date of publication September 7, 2021, date of current version September 17, 2021.

Digital Object Identifier 10.1109/ACCESS.2021.3110876

Joint Bernoulli Filtering and MIMO Processing for Detection of Moving Targets in Shallow Ocean Environments

HUANGYU DAI[1], XIANG PAN[1], ZHONGDI LIU[1], PENG ZHANG[1], AND ZHONGYONG CHEN[2]

[1]School of Information Science and Electronic Engineering, Zhejiang University, Hangzhou 310027, China
[2]Zhejiang Medical Products Administration, Hangzhou 310012, China

Corresponding author: Xiang Pan (panxiang@zju.edu.cn)

The work of Xiang Pan was supported in part by the National Natural Science Foundation of China under Grant 41776108, Grant 61571397, and Grant 61171148; and in part by the National Key Research Program of China under Grant 2017YFC0306901.

ABSTRACT A joint multiple-input multiple-output (MIMO) processing framework is proposed to exploit spatial diversity and moving cues for the enhancement of target detection in a shallow ocean environment. Orthogonal signals are transmitted to illuminate different aspects of a target and beamforming operation is carried out over the received data for estimating target bearing. The target range is achieved by a replica correlation integrator where the beamformer outputs are matched with transmitted signals. After meanshift clustering algorithm is carried out over the bearing-range spectrums to generate the clutter centers, the potential trajectories of targets can be tracked by an improved Bernoulli filter with inputs of these centers. The at-sea experimental results have shown the effectiveness of the joint processing framework in MIMO detection of moving targets.

INDEX TERMS MIMO detection, Bernoulli filtering, spatial diversity, moving target, sea trial.

I. INTRODUCTION

Detection of underwater targets is a challenging task in shallow ocean environments due to multipath propagation resulting in time-delay spread of waveforms. The performance of passive sonar is limited in detection of quiet targets when their abient signals are buried in ocean background noise. Meanwhile, active detection faces the challenge of strong bottom reverberation resulting in a low echo-to-reverberation ratio and lots of clutter interferences. Multiple-input multiple-output (MIMO) processing framework attracts a great deal of interest in radar and sonar due to taking advantage of spatial diversity for the enhancement of target detection. Based on our previous work on MIMO detection, this paper focuses on the detection [1]–[3] of underwater moving targets using an improved Bernoulli filtering algorithm. The proposed framework can effectively reduce the probability of false alarms and improve the detection ability of underwater moving targets, and it can also be used in other fields to detect moving targets in the same way.

The associate editor coordinating the review of this manuscript and approving it for publication was Liang Yang.

MIMO technology was first applied in a wireless communication system to suppress channel fading through MIMO devices [4], [5]. In 2004, Fishler proposed the MIMO detection concept based on the complete diversity of transceivers [6]. Then, many achievements on MIMO radar had been realized. In the next few years, for instance, the Colocated MIMO system [7], [8] was utilized by Hack to detect static targets [9], while the distributed MIMO [10] was further proposed by Li to detect moving targets [11], which performs much better than the traditional sonar system in target localization.

Due to the maturity of MIMO radar technology, MIMO sonar technology develops rapidly. MIMO sonar was investigated by Bekkerman on detection and localization of targets in [12], where the Cramér-Rao lower bound was derived for target bearing estimation. A perceptual MIMO sonar processing model was proposed by Lynch *et al.* [13] to improve robustness of MIMO detection algorithms. Vossen *et al.* focused on the dense sampling processing method of MIMO sonar data and improved the target detection ability by introducing the virtual array source [14]. However, currently distributed MIMO sonar [15] is mainly used for detection

and positioning of stationary targets [1], [2]. The framework proposed in this paper focuses on detection of motion targets.

The target moving clue can be utilized for enhancing detection of weak targets, which is called tracking before detection (TBD). A traditional tracking system includes three parts: target detection, data association, and tracking filtering.

The Kalman filter (KF) [16], a classic single target tracking algorithm, was first proposed in 1960 by Rudolph E.Kalman to model the targets' state space and measurement space under linear Gaussian assumption. The extended Kalman filter (EKF), the unscented Kalman filter (UKF), and the particle filter (PF) are widely utilized in a nonlinear Gaussian situation. In our latest article, the cubature Kalman filter (CKF) [17] and adaptive current statistical (ACS) model was shown to be better for tracking maneuvering targets [18]. In this paper, CKF is also deployed to track underwater targets for the benefit of its lower complexity and better stability.

The data association approach is commonly utilized in multiple target tracking for reduction of false alarm probability in active sonar detection. Nearest neighbor (NN), probabilistic data association (PDA), joint probabilistic data association (JPDA), and multiple hypothesis tracking (MHT) are mainstream methods in data association.

Filtering algorithm based on random finite set (RFS) theory and Bayesian framework is a new technology to solve multi-target tracking in clutter environments [19], which focuses on the target state in measurement sets instead of paying attention to the data association step. Since RFS cannot be calculated directly, probability hypothesis density (PHD) is proposed as an approximation approach to propagate the first-order moment of target probability density [20]. The cardinalized PHD (CPHD) modifies the PHD by propagating the entire distribution to get a more stable and accurate estimation of target number [21]. Different from the PHD and CPHD filters, the multi-target multi-Bernoulli (MeMBer) filter was proposed by Mahler [22] to propagate the multi-target posterior density, while it suffers from the overestimation of cardinality (number of targets). The cardinality balanced multi-target multi-Bernoulli (CBMEMBer) filter was proposed by Ba-Tuong Vo to overcome the bias problem [23]. Also, to mark each trajectory, Ba-Ngu Vo *et al* proposed labeled RFSs [24] and deduced generalized labeled multi-Bernoulli (GLMB) and δ-GLMB filters [25], [26]. Recently, the detection and tracking work based on improved Bernoulli filtering is widely investigated and applicable across a broad range of domains [27]–[31].

The main contributions of this paper are as follows:

(1) A processing framework based on combination of MIMO sonar and Bernoulli filter is proposed to exploit target diversity and moving cues for the enhancement of target detection in shallow ocean environments. A replica correlation integrator (RCI) [32] is utilized to replace the traditional matched filter for alleviating distance ambiguity caused by multipath in shallow ocean environments.

(2) To meet the requirement of Bernoulli filter's hypothesis that each measurement can only correspond to one target and vice versa, a series of transformations, including generalized likelihood ratio test (GLRT) estimator and meanshift clustering [33], [34] are developed in bearing-range spectrums to extract the valid measurement set. A new filter called δ-cardinality balanced generalized labeled multi-Bernoulli (δ-CBGLMB) filter is proposed to improve the detection ability with a lower computational cost. It first extracts part of the measurement sets through the traditional CBMEMBer filter and then uses the GLMB filter to track targets.

(3) A sea trial is designed to verify the effectiveness of combination of the distributed MIMO and δ-CBGLMB filter for detection of small targets in shallow water environments. The experimental results have shown that the target can be detected in reverberant environments due to exploiting target diversity and moving clues. The result of the sea trial validates the effectiveness of the distributed MIMO detection framework, and the relevant experimental research has not been done before.

The structure of this paper is as follows. In Section II, the technology in distributed MIMO is presented. In Section III, meanshift clustering algorithm is presented to extract measurement sets over bearing-range spectrums. In Section IV, Bernoulli filter is introduced to find out potential trajectories of expected targets. The sea trial is briefly described, and the experiment results are shown in Section V. Conclusions are given in Section VI.

II. DISTRIBUTED MIMO

The concept of MIMO has been presented for many years, the simplest MIMO system can be modeled by $\bar{r} = \bar{H}\bar{s} + \bar{n}$, where $\bar{H}$ represents the channel response, $\bar{s}$ represents the transmit signals, $\bar{n}$ is noise and $\bar{r}$ is the received signals [15]. The expression above shows that a complete MIMO system needs suitable transmit signal, numbers of transmitters and receivers. Therefore $\bar{H}$ contains multiple path components when the MIMO system is implemented to a shallow ocean environment.

A. GENERALIZED LIKELIHOOD RATIO TEST DETECTOR

A suitable model considering shallow ocean multipaths and Doppler is established as follows:

$$\mathbf{y}_n^{ij} = \gamma_t^{ij} e^{\mathcal{J}\theta_n^{ij}(\mathbf{t})} D_t^{ij} \mathbf{s}^i + \mathbf{n}_n^{ij}, \tag{1}$$

where $\mathbf{y}_n^{ij} \in \mathbb{C}^{L\times 1}$ represents the signal from the ith sound source received by nth array element on jth receiver, L represents the snapshot of the signal, $\mathbf{s}^i \in \mathbb{C}^{L\times 1}$ is the signal of ith sound source, the term $\mathbf{n}_n^{ij} \in \mathbb{C}^{L\times 1}$ contains reverberation and noise. To simplify the derivation, it is assumed to be independent identically distributed (IID) Gaussian noise with $\mathcal{N}\left(\mathbf{0}_L, \sigma^2\mathbf{I}_L\right)$, $D_t^{ij} = D\left(\tau_t^{ij}, \nu_t^{ij}\right) \in \mathbb{C}^{L\times L}$ is Doppler time delay factor of ith transmitter and jth receiver. $\theta_n^{ij}(\mathbf{t})$ is the phase difference of the nth array element relative to the reference array element under the plane wave model. Specific

definition of $\theta_n^{ij}(\mathbf{t})$ and $\theta_n^{ij}(\mathbf{t})$ are

$$\theta_n^{ij}(\mathbf{t}) = \left(\frac{2\pi}{\lambda^i}\right)\hat{\mathbf{k}}^j(\mathbf{t})\cdot\mathbf{d}_n^j, \tag{2}$$

$$\mathbf{D}(\tau,\nu) = \mathbf{D}_L\left(\nu/f_s\right)\mathbf{W}^H\mathbf{D}_L\left(-\tau f_s/L\right)\mathbf{W}, \tag{3}$$

where $\mathbf{D}_L(x) = \text{diag}\left(\left[e^{\mathcal{J}2\pi(0)x},\cdots,e^{\mathcal{J}2\pi(L-1)x}\right]\right) \in \mathbb{C}^{L\times L}$, $\mathbf{W}$ is unitary discrete fourier transform matrix.

Supposing that each array has N_e array number, combining them, then the model can be written as follows:

$$\mathbf{y}^{ij} = \gamma_t^{ij}\left(\mathbf{a}_t^{ij}\otimes D_t^{ij}\right)\mathbf{s}^i + \mathbf{n}^{ij}, \tag{4}$$

where $\mathbf{a}^{ij}(\mathbf{t}) = \left[e^{\mathcal{J}\theta_1^{ij}(\mathbf{t})},\cdots,e^{\mathcal{J}\theta_{N_e}^{ij}(\mathbf{t})}\right]^T \in \mathbb{C}^{N_e\times 1}$ is the Kronecker product, $\mathbf{y}^{ij} = \left[\left(\mathbf{y}_1^{ij}\right)^T,\cdots,\left(\mathbf{y}_{N_e}^{ij}\right)^T\right]^T \in \mathbb{C}^{N_eL\times 1}$,

Considering that the target appears in the detection unit $(p,\dot{p})$, where p and $\dot{p}$ represent target speed and position respectively, the binary hypothesis test is

$$\begin{aligned}\mathcal{H}_1 &: \mathbf{y}^{ij} = \gamma_p^{ij}\left(\mathbf{a}_p^{ij}\otimes D_p^{ij}\right)\mathbf{s}^i + \mathbf{n}^{ij}\\ \mathcal{H}_0 &: \mathbf{y}^{ij} = \mathbf{n}^{ij}.\end{aligned} \tag{5}$$

Setting $\mathbf{y}^i = \left[\left(\mathbf{y}^{i1}\right)^T,\cdots,\left(\mathbf{y}^{iN_r}\right)^T\right]^T$, which represents the measurement of the ith sound source of the receiver, $\mathbf{y} = \left[\left(\mathbf{y}^1\right)^T,\cdots,\left(\mathbf{y}^{N_r}\right)^T\right]^T$ represents all measurements in a distributed system, $\gamma_p^i = \left[\gamma^{i1},\cdots,\gamma^{iN_r}\right]^T$ is the propagation coefficient related to the ith sound source, $\gamma_p = \left[\left(\gamma_p^1\right)^T,\cdots,\left(\gamma_p^{N_t}\right)^T\right]^T$ is the whole propagation coefficient, $\mathbf{s} = \left[\left(\mathbf{s}^1\right)^T,\cdots,\left(\mathbf{s}^{N_t}\right)^T\right]^T$ represents all transmitting signals, N_t and N_r are the number of transmitters and receivers respectively.

Based on the hypothsis that the noise received is IID and $\mathbf{s}$ and γ_p are unknown, they can be replaced by using maximum likelihood estimates (MLE), which is called GLRT. The GLRT detector is

$$\sum_{i=1}^{N_t}\lambda_1\left(\Phi^i\Phi^{iH}\right)\underset{\mathcal{H}_1}{\overset{\mathcal{H}_1}{\gtrless}}\kappa. \tag{6}$$

where $\Phi^i = \left[\tilde{\mathbf{y}}_b^{i1},\cdots,\tilde{\mathbf{y}}_b^{iN_r}\right] \in \mathbb{C}^{N_r\times L}$, $\mathbf{y}_b^{ij} = \frac{1}{\sqrt{N_e}}\sum_{n=1}^{N_r}\left[\mathbf{a}_p^{ij}\right]_n^*\mathbf{y}_n^{ij}$, κ is determined by false alarm rate (FAR), $\lambda_1(\cdot)$ represents the largest eigenvalue of the matrix. See Appendix for specific derivation.

The specific implementation process of GLRT detector: The monitoring area is divided into grids in a two-dimensional space. According to the received data, (6) is used to obtain the maximum likelihood value of each cell to form a likelihood value plane. Then, set a threshold to extract the likelihood plane position that is greater than the threshold. The algorithm is shown in Fig. 1.

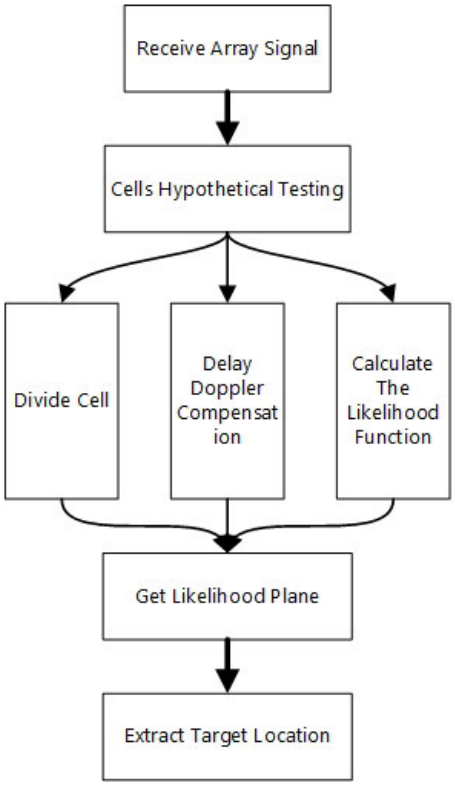

FIGURE 1. GLRT estimation flowchart.

B. REPLICA CORRELATION INTEGRATION

In radar and sonar, matched filter is commonly used to find the signal of interest by maximizing the signal-to-noise (SNR) of its output. Supposing the noise in the MIMO model is Gaussian white noise, the impulse response of matched filter can be produced as follows:

$$h(t) = ks^*\left(t_0 - t\right), \tag{7}$$

where $*$ is conjugate, t_0 is the delay. It can be seen from (7) that the replica is the conjugated and time-reverse version of the transmitted signal with a time-delay.

Due to time spreading distortion in shallow ocean environment,the received echo should be modeled as a convolution of the transmit signal with a time spreading function $p(t)$ [32].

$$x(t) = \frac{a}{\sqrt{f_sT_s}}\sum_{i=0}^{f_sT_s-1}p(i)\,s\left(t-t_0-i\right) \tag{8}$$

where a denotes the echo attenuation, f_s is the sample rate and T_s is the length of $p(t)$.

In [32], the Replica Correlation Integration (RCI) detector is proposed to mitigate the effect of multipath.

$$y(t) = \sum_{k=0}^{M-1}\left|\sqrt{\frac{2}{N}\sum_{i=0}^{N-1}s^*(i-k)\,x(t+i)}\right|^2 \tag{9}$$

where $M = T_sf_s$, $y(t)$ is matched filtering output.

III. MEANSHIFT CLUSTERING

Through the spatial-temporal matched filtering, the bearing-range spectrum is generated which contains potential targets and a great deal of clutters. Due to the low resolution of the spectrum, Bernoulli filtering cannot directly be utilized for tracking targets. Therefore, meanshift clustering algorithm is implemented to extract a valid measurement set.

Considering about a set of N IID n-dimensional random vectors $X_1, X_2, \cdots, X_N$, the form of multivariate kernel density estimators is proposed by Cacoullos *et al* [33].

$$\hat{f}_N(X) \equiv \left(Nh^n\right)^{-1} \sum_{i=1}^{N} s\left(h^{-1}\left(X - X_j\right)\right), \tag{10}$$

where $s(X)$ is a scalar function and it needs to satisfy some rules, which is given in [34]. h is a function of the sample size N. Then, the differentiable kernel function is used to get the density gradient estimate.

$$\hat{\nabla}_x f_N(X) = \left(Nh^{n+1}\right)^{-1} \sum_{j=1}^{N} \nabla s\left(h^{-1}\left(X - X_j\right)\right), \tag{11}$$

where

$$\nabla s(Y) \equiv \left(\frac{\partial s(Y)}{\partial y_1}, \frac{\partial s(Y)}{\partial y_2}, \cdots, \frac{\partial s(Y)}{\partial y_n}\right)^T. \tag{12}$$

The scaler fuction here uses Gaussian probablity density kernel function.

$$s(X) \equiv \frac{\exp\left(-\frac{1}{2}X^T X\right)}{(2\pi)^{n/2}} \tag{13}$$

substituting (13) into (11), the estimate of the gradient density becomes

$$\hat{\nabla}_x f_N(X) = N^{-1} \sum_{i=1}^{N} (X_i - X)(2\pi)^{-n/2} h^{-(n+2)} \cdot \exp\left[-(X - X_i)^T \left(\frac{X - X_i}{2h^2}\right)\right]. \tag{14}$$

Meanshift clustering algorithm uses gradient descent to get the center of each bright spot. The form of meanshift gradient descent can be written as

$$X_j^{k+1} = X_j^k + \alpha \hat{\nabla}_x \ln f_N\left(X_j^k\right), \tag{15}$$

the specific process of meanshift clustering is shown in Algorithm 1.

IV. BERNOULLI FILTER

In the case of a low SNR ratio, there are a huge amount of peaks in the ambiguity plane generated by spatial-temporal matched filtering which results in large false alarms and a large probability of miss-detection. Therefore, a TBD algorithm is proposed in this section for target detection based on Bernoulli filtering. The Bernoulli filter is built on the RFS theory which is suitable for solving the uncertainty detection issue.

Algorithm 1 Meanshift Clustering Algorithm

Input: Position set of bright spots in each frame, $Z_{initial}$; Bandwidth, B; Stop thresh, T; Learning rate, α;

Output: Center of each bright spot, Z_{final};

1: Randomly select a point in $Z_{initial}$ as center point X_j^k;
2: Find all points within the bandwidth B from the center point and record it as set M;
3: Compute the gradient density $\hat{\nabla}_x f_N(X)$ using (14) and compare with stop thresh T, if $\hat{\nabla}_x f_N(X) > T$, continue; else, jump to state 5;
4: Update the center point using (15) and jump back to step 2;
5: Compute $Z_{final} = Z_{final} \cup X_j^k$, $Z_{initial} = Z_{initial} \cap M$;
6: Determine whether $Z_{initial} = \varnothing$, if $Z_{initial} = \varnothing$, **return** Z_{final}; else, jump back to step 1;

A. MULTI-TARGET MULTI-BERNOULLI FILTER

The MeMBer filter [22] is a commonly used Bernoulli filter. It approximates the multi-objective state set at each moment with a multi-Bernoulli RFS, and it must follow some modeling assumptions that each target or clutter state is independent of each other, target births follow a multi-Bernoulli RFS, and clutter follows a Poisson RFS. The MeMBer recursion also can be divided into two steps like Bayes recursion.

In model prediction step, suppose that at time $j-1$ the target state RFS is $\mathbf{T}_{j-1}$, there are two options for each target, survive with a probability of $p_{S,j}\left(\mathbf{t}_{j-1}\right)$ and moves to a new state with probablity density $f_{j|j-1}\left(\mathbf{t}_j|\mathbf{t}_{j-1}\right)$, or die with a probability of $1 - p_{S,j}\left(\mathbf{t}_{j-1}\right)$. The multi-target state $\mathbf{T}_j$ can be represented as

$$\mathbf{T}_j = \mathbf{B}_j \cup \left(\bigcup_{\mathbf{t}_{j-1} \in \mathbf{T}_{j-1}} \mathbf{S}_{j|j-1}\left(\mathbf{t}_{j-1}\right)\right), \tag{16}$$

where $\mathbf{S}_{j|j-1}\left(\mathbf{t}_{j-1}\right)$ is the RFS representation of the state at the next time, $\mathbf{B}_j$ is the RFS of spontaneous birth. So, suppose that at time $j-1$, the form of the posterior multi-target density is

$$\chi_{j-1} = \left\{\left(r_{j-1}^{(i)}, p_{j-1}^{(i)}\right)\right\}_{i=1}^{M_{j-1}}. \tag{17}$$

Then the form of predicted multi-target density is

$$\chi_{j|j-1} = \left\{\left(r_{P,j|j\text{-}1}^{(i)}, p_{P,j|j-1}^{(i)}\right)\right\}_{i=1}^{M_{j-1}} \bigcup \left\{\left(r_{B,j}^{(i)}, p_{B,j-1}^{(i)}\right)\right\}_{i=1}^{M_{B,j}}, \tag{18}$$

where

$$r_{P,j|j-1}^{(i)} = r_{j-1}^{(i)} \left\langle p_{j-1}^{(i)}, p_{S,j} \right\rangle, \tag{19}$$

$$p_{P,j|j-1}^{(i)}\left(\mathbf{t}\right) = \frac{\left\langle f_{k|k-1}\left(\mathbf{t}|\cdot\right), p_{P,j|j-1}^{(i)} p_{S,j} \right\rangle}{\left\langle p_{j-1}^{(i)}, p_{S,j} \right\rangle}, \tag{20}$$

$\langle v, h \rangle = \int v(t)h(t)dt$.

In state update step, suppose that the target RFS is $\mathbf{T}_j$ at time j, there are also two options for each target, detected

with a probability of $p_{D,j}\left(\mathbf{t}_j\right)$ and combine with likelihood $g_j\left(\mathbf{m}_j|\mathbf{t}_j\right)$ to generate a measurement $\mathbf{m}_k$ or missed with a probability of $1-p_{D,j}\left(\mathbf{t}_j\right)$. And a set of false alarms and clutter can be modeled as Poisson RFSs K_j. The measurement set can be represented as

$$\mathbf{M}_j = \left(\bigcup_{\mathbf{t}_j\in\mathbf{T}_j}\Theta_j\left(\mathbf{t}_j\right)\right)\cup\mathbf{K}_j, \tag{21}$$

where $\Theta_j\left(\mathbf{t}_j\right)$ is the situation of detection. If $\Theta_j\left(\mathbf{t}_j\right)=\mathbf{m}_j$, it means that the MIMO system detects the target. Or else $\Theta_j\left(\mathbf{t}_j\right)=\varnothing$, it means that the MIMO doesn't find the target. Suppose at time j, the form of the predicted multi-target density is

$$\chi_{j|j-1}=\left\{\left(r_{j|j-1}^{(i)},p_{j|j-1}^{(i)}\right)\right\}_{i=1}^{M_{j|j-1}}. \tag{22}$$

Then the form of posterior multi-target density can be approximated as follows:

$$\chi_j\approx\left\{\left(r_{L,j}^{(i)},p_{L,j}^{(i)}\right)\right\}_{i=1}^{M_{j|j-1}}\bigcup\left\{\left(r_{U,j}(\mathbf{m}),p_{U,j}(\cdot;\mathbf{m})\right)\right\}_{\mathbf{m}\in\mathbf{m}_j}, \tag{23}$$

where

$$r_{L,j}^{(i)}=\frac{r_{j|j-1}^{(i)}\left(1-\left\langle p_{j|j-1}^{(i)},p_{D,j}\right\rangle\right)}{1-r_{j|j-1}^{(i)}\left\langle p_{j|j-1}^{(i)},p_{D,j}\right\rangle}, \tag{24}$$

$$p_{L,j}^{(i)}(\mathbf{t})=\frac{p_{j|j-1}^{(i)}(\mathbf{t})\left(1-p_{D,j}(\mathbf{t})\right)}{1-\left\langle p_{j|j-1}^{(i)},p_{D,j}\right\rangle}, \tag{25}$$

$$r_{U,j}(\mathbf{m})=\frac{\sum_{i=1}^{M_{j|j-1}}\frac{r_{j|j-1}^{(i)}\left\langle p_{j|j-1}^{(i)},\psi_{j,\mathbf{m}}\right\rangle}{1-r_{j|j-1}^{(i)}\left\langle p_{j|j-1}^{(i)},p_{D,j}\right\rangle}}{\kappa_j(\mathbf{m})+\sum_{i=1}^{M_{j|j-1}}\frac{r_{j|j-1}^{(i)}\left\langle p_{j|j-1}^{(i)},\psi_{j,\mathbf{m}}\right\rangle}{1-r_{j|j-1}^{(i)}\left\langle p_{j|j-1}^{(i)},p_{D,j}\right\rangle}}, \tag{26}$$

$$p_{U,j}(\mathbf{t};\mathbf{m})=\frac{\sum_{i=1}^{M_{j|j-1}}\frac{r_{j|j-1}^{(i)}p_{j|j-1}^{(i)}(\mathbf{t})\psi_{j,\mathbf{m}}(\mathbf{t})}{1-r_{j|j-1}^{(i)}\left\langle p_{j|j-1}^{(i)},p_{D,j}\right\rangle}}{\sum_{i=1}^{M_{j|j-1}}\frac{r_{j|j-1}^{(i)}\left\langle p_{j|j-1}^{(i)},\psi_{j,\mathbf{m}}\right\rangle}{1-r_{j|j-1}^{(i)}\left\langle p_{j|j-1}^{(i)},p_{D,j}\right\rangle}}, \tag{27}$$

$\psi_{j,\mathbf{m}}(\mathbf{t})=g_j\left(\mathbf{m}|\mathbf{t}\right)p_{D,j}\left(\mathbf{t}\right)$.

The traditional MeMBer filter always meets the problem of overestimation of cardinality. So CBMEMBer filter was proposed by Ba-Tuong Vo *et al* in [23]. It only changes the approximated form of posterior multi-target density as

$$\chi_j\approx\left\{\left(r_{L,j}^{(i)},p_{L,j}^{(i)}\right)\right\}_{i=1}^{M_{j|j-1}}\cup\left\{\left(r_{U,j}^{*}(\mathbf{m}),p_{U,j}^{*}(\cdot;\mathbf{m})\right)\right\}_{\mathbf{m}\in\mathbf{M}_j}, \tag{28}$$

where

$$r_{U,j}^{*}(\mathbf{m})=\frac{\sum_{i=1}^{M_{j|j-1}}\frac{r_{j|j-1}^{(i)}\left(1-r_{j|j-1}^{(i)}\right)\left\langle p_{j|j-1}^{(i)},\psi_{j,\mathbf{m}}\right\rangle}{\left(1-r_{j|j-1}^{(i)}\left\langle p_{j|j-1}^{(i)},p_{D,j}\right\rangle\right)^2}}{\kappa_j(\mathbf{m})+\sum_{i=1}^{M_{j|j-1}}\frac{r_{j|j-1}^{(i)}\left\langle p_{j|j-1}^{(i)},\psi_{j,\mathbf{m}}\right\rangle}{1-r_{j|j-1}^{(i)}\left\langle p_{j|j-1}^{(i)},p_{D,j}\right\rangle}}, \tag{29}$$

$$p_{U,j}^{*}(\mathbf{t};\mathbf{m})=\frac{\sum_{i=1}^{M_{j|j-1}}\frac{r_{j|j-1}^{(i)}}{1-r_{j|j-1}^{(i)}}p_{j|j-1}^{(i)}(\mathbf{t})\psi_{j,\mathbf{m}}(\mathbf{t})}{\sum_{i=1}^{M_{j|j-1}}\frac{r_{j|j-1}^{(i)}}{1-r_{j|j-1}^{(i)}}\left\langle p_{j|j-1}^{(i)},\psi_{j,\mathbf{m}}\right\rangle}. \tag{30}$$

B. LABELED MULTI-BERNOULLI FILTER

The δ-generalized labeled multi-Bernoulli (δ-GLMB) filter [25] is introduced in this subsection, which will be combined with CBMEMBer filter to get a better result in distributed MIMO detection system.

δ-GLMB is a solution to labeled RFS [24], the form of labeled RFS is $\boldsymbol{\chi}\left(\left\{\left(\mathbf{t}_1,\ell_1\right),\ldots,\left(\mathbf{t}_n,\ell_n\right)\right\}\right)$, where $\ell\in\mathbb{L}$ is the label space. Based on the form of labeled RFS, δ-GLMB can be written as follows:

$$\chi(\mathbf{T})=\Delta(\mathbf{T})\sum_{(I,\xi)\in\mathcal{F}(\mathbb{L})\times\Xi}\omega^{(I,\xi)}\delta_I(\mathcal{L}(\mathbf{T}))\left[p^{(\xi)}\right]^{\mathbf{T}}, \tag{31}$$

where $\Delta(\mathbf{T})\triangleq\delta_{|\mathbf{T}|}(|\mathcal{L}(\mathbf{T})|)$ denotes the distinct label indicator, $\mathcal{L}(\mathbf{T})=\{\mathcal{L}(\mathbf{t}):\mathbf{t}\in\mathbf{T}\}$, $\mathcal{L}((\mathbf{t},\ell))=\ell$ is the label of set $\mathbf{T}$, $\xi\in\Theta_{0:j}$ represents a history of association maps before $j+1$, $\Theta_{0:j}\triangleq\Theta_0\times\cdots\times\Theta_j$, $\omega^{(I,\xi)}=w^{(\xi)}(I)$ represents the probability of each label track set and $p^{(\xi)}$ is the probability density.

In model prediction step, suppose that the form of the posterior multi-target density is (31), then the prediction multi-target density is

$$\begin{aligned}&\boldsymbol{\chi}_+\left(\mathbf{T}_+\right)\\&=\Delta\left(\mathbf{T}_+\right)\sum_{(I_+,\xi)\in\mathcal{F}(\mathbb{L}_+)\times\Xi}\omega_+^{(I_+,\xi)}\delta_{I_+}\left(\mathcal{L}\left(\mathbf{T}_+\right)\right)\left[p_+^{(\xi)}\right]^{\mathbf{T}+},\end{aligned} \tag{32}$$

where

$$\omega_+^{(I_+,\xi)}=\omega_S^{(\xi)}\left(I_+\cap\mathbb{L}\right)w_B\left(I_+\cap\mathbb{B}\right), \tag{33}$$

$$\omega_S^{(\xi)}(L)=\left[\eta_S^{(\xi)}\right]^L\sum_{I\supseteq L}\left[1-\eta_S^{(\xi)}\right]^{I-L}\omega^{(I,\xi)}, \tag{34}$$

$$\eta_S^{(\xi)}(\ell)=\left\langle p_S(\cdot,\ell),p^{(\xi)}(\cdot,\ell)\right\rangle, \tag{35}$$

$$p_+^{(\xi)}(\mathbf{t},\ell)=1_{\mathbb{L}}(\ell)p_S^{(\xi)}(\mathbf{t},\ell)+1_{\mathbb{B}}(\ell)p_B(\mathbf{t},\ell), \tag{36}$$

$$p_S^{(\xi)}(\mathbf{t},\ell)=\frac{\left\langle p_S(\cdot,\ell)f\left(\mathbf{t}\mid\cdot,\ell\right),p^{(\xi)}(\cdot,\ell)\right\rangle}{\eta_S^{(\xi)}(\ell)}, \tag{37}$$

$\mathbb{L}\triangleq\mathbb{L}_{0:j}$ represents the label space before time $j+1$, $\mathbb{B}\triangleq\mathbb{B}_{j+1}$ represents the label space in $j+1$, w_S and w_B are the weight of survival and new birth probability respectively.

In state update step, also suppose that the form of the predicted multi-target density is (31). Then the prediction multi-target density is

$$\begin{aligned}\chi(\mathbf{T}|M)=\Delta(\mathbf{T})&\sum_{(I,\xi)\in\mathcal{F}(L)\times\Xi}\sum_{\theta\in\Theta(I)}\omega^{(I,\xi,\theta)}(M)\delta_I(\mathcal{L}(\mathbf{T}))\\&\times\left[p^{(\xi,\theta)}(\cdot\mid M)\right]^{\mathbf{T}},\end{aligned} \tag{38}$$

where

$$\omega^{(I,\xi,\theta)}(M) \propto \omega^{(I,\xi)}\left[\eta_M^{(\xi,\theta)}\right]^I, \tag{39}$$

$$\eta_M^{(\xi,\theta)}(\ell) = \left\langle p^{(\xi)}(\cdot,\ell), \psi_M(\cdot,\ell;\theta)\right\rangle, \tag{40}$$

$$p^{(\xi,\theta)}(\mathbf{t},\ell \mid M) = \frac{p^{(\xi)}(\mathbf{t},\ell)\psi_M(\mathbf{t},\ell;\theta)}{\eta_M^{(\xi,\theta)}(\ell)}, \tag{41}$$

$$\begin{aligned}\psi_M(\mathbf{t},\ell;\theta) = {} & \delta_0(\theta(\ell))q_D(\mathbf{t},\ell) \\ & + (1-\delta_0(\theta(\ell)))\frac{p_D(\mathbf{t},\ell)g\left(m_{\theta(\ell)} \mid t,\ell\right)}{\kappa\left(m_{\theta(\ell)}\right)},\end{aligned} \tag{42}$$

I represents a set of track labels, $\Theta(I)$ is association maps in I, $q_D(\mathbf{t},\ell) = 1 - p_D(\mathbf{t},\ell)$.

The traditional δ-GLMB algorithm is intractable because of a large number of data associations and tracks assumptions. δ-GLMB deploys K-shortest path algorithm [35] and Bellman-Ford [36] algorithm to solve the associations between each time, Murty's algorithm is used to link the predict targets with measurement sets [37]. Although the above algorithms can reduce the computational cost, the computational cost of δ-GLMB filter is still huge.

In this paper, the advantage of traditional Bernoulli and label Bernoulli are combined to extract targets more accurately and efficiently. The cardinality is doubled compared to the CBMEMBer filter, and then the measurement sets of potential targets by the CBMEMBer filter are extracted. Finally, the δ-GLMB filter imports the new measurement sets to predict the target trajectory. This new filter is named δ- cardinality balanced generalized labeled multi-Bernoulli (δ-CBGLMB), which can reduce the computational cost and extract more accurate trajectories for potential targets. It reduces the number of measurements through the CBMEMBer filter, which can reduce the amount of calculation of the ranked assignment problem in the δ-GLMB filter. The complexity of the GLMB assignment problems is $O\left(T|Z|^3\right)$, where T represents the number of assignments, $|Z|$ represent the number of measurements, so this new filter can effectively reduce the complexity of the δ-GLMB filter. The performance of δ-CBGLMB is shown in Section V.

V. SEA TRIAL

In order to verify the effectiveness and practicality of the distribution MIMO detection framework, MIMO experiments are carried out in Zhoushan sea ares in August, 2020. It is seen from Fig. 2 that the speed of sound does not change with depth (yellow line). Here, the black curve denotes the temperature change of water volume.

A. SYSTEM DESIGN OF SEA TRIAL

The system can divide into three parts: transmitter system; targets; receiver system. The Transmitter system includes a NI transmitter, an 8-channel power amplifier, a high power amplifier, and two 2-element transmit arrays. The NI device generates two signals at the same time, which are input to two transmit sub-arrays after passing the 8-channel power amplifier and the high power amplifier respectively, the two transmit sub-arrays are arranged at 8m underwater; the Receiver system includes a NI receiver and a 16 elements horizontal uniform linear array with an array spacing of 0.075m, which is arranged at 7m underwater; The two targets are approximately 6.5m below the water surface. Some details about the environment and the system design are shown in Fig. 3.

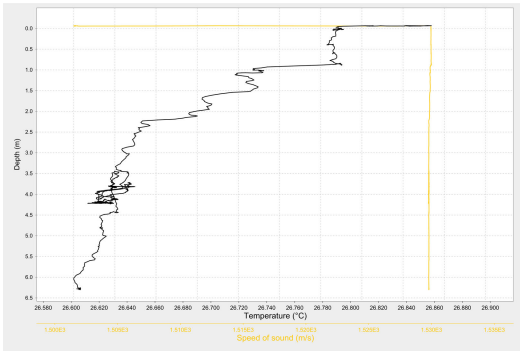

FIGURE 2. Sound velocity gradient.

B. TARGET DETECTION AND TRACKING

The targets are two cylinders with a bottom diameter of 50 cm and a length of about 4 m. They are hung on two sub-ships, and two sub-ships move in the direction away from the mastership. Each experiment lasted for 400s, and $6-10$kHz and $10-14$kHz LFM signals with fixed bandwidth are transmitted every 1s. After multiple sets of experiments, the targets can be detected most of the time when transmitting the conventional LFM signal; the targets can only be detected in a small amount of time when transmitting coded LFM signal. Therefore, the subsequent processing and analysis of the experimental results are based on the conventional orthogonal LFM signal with a pulse width of 20ms.

Several sets of bearing-range spectrums are extracted for analysis. Due to experimental conditions, two power amplifiers with different power amplification multiples are used. The left sub-array here corresponds to the relatively low power amplifier, and the right sub-array here corresponds to the relatively high power amplifier. In Fig. 4 and Fig. 5, It can be clearly seen that the detection capabilities of the left and right sub-arrays are completely different, depending on the relative positions of the two transmitting arrays and the two targets. In bearing-range spectrum 260 and 271, only the left sub-array in bearing-range spectrum 260 and the right sub-array in bearing-range spectrum 271 can identify the two targets. However, two targets can be found clearly in the MIMO bearing-range spectrum by combining the left and the right bearing-range spectrum under incoherent conditions. It can be well proved that the distributed MIMO framework helps improve detection capabilities because clutter measurements are uncorrelated, while target measurements are related. Observing subfigure (a) and (c) in Fig. 4 and Fig. 5,

FIGURE 3. Sea trial design: (a) Diagram of experimental scene; (b) Underwater target; (c) Sub-ship.

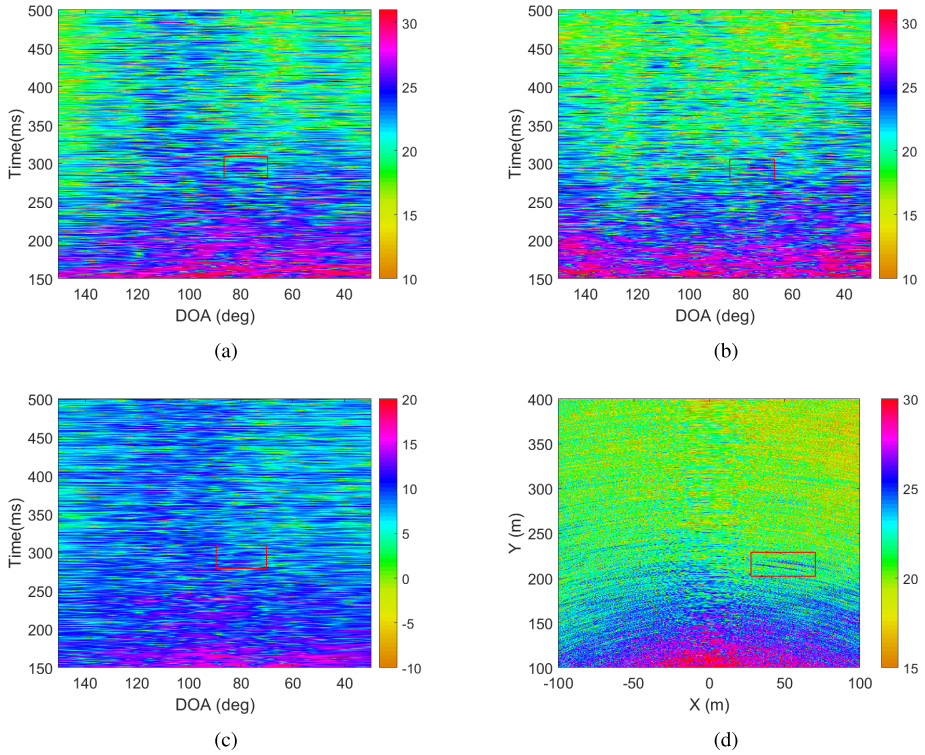

FIGURE 4. bearing-range spectrum 260: (a) Left sub-array; (b) Right sub-array; (c) Left sub-array using RCI; (d) MIMO.

it is evident that the inconspicuous targets have become evident in bearing-range spectrum 271 after using RCI, but it requires extra computational cost in performing RCI. The target's resolution in the distance dimension reduces, and the computation cost has increased a lot. Meanwhile, in bearing-range spectrum 260, the initially clear targets become blurred. It means that when the RCI parameters do not match the actual environment, RCI may obscure the original target and increase the probability of missed detection.

After drawing each bearing-range spectrum, the near-field reverberation should be removed, the threshold should be set to extract observation set blocks and the meanshift algorithm should be performed to obtain cluster centers, which are required by Bernoulli filter. The results of meanshift clustering are shown in Fig. 6. In the measurement set extraction process, selecting the correct threshold, eliminating the near-field reverberation, and setting the bandwidth of the meanshift clustering algorithm are the keys to extracting the measurement set. In this paper, some parameter setting suggestions are given. The threshold value needs to be changed according to different ranges. It is better to choose a threshold slightly larger than the amplitude under the same range. When removing the near field reverberation area, the relatively low power sub-array should be considered first. The bandwidth

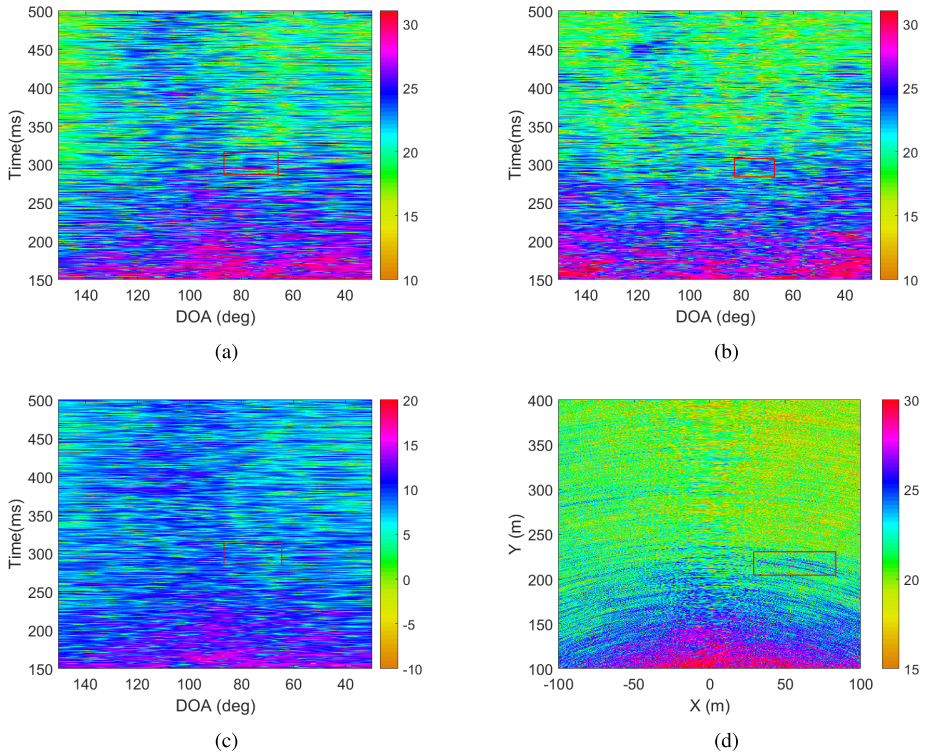

FIGURE 5. bearing-range spectrum 271: (a) Left sub-array; (b) Right sub-array; (c) Left sub-array using RCI; (d) MIMO.

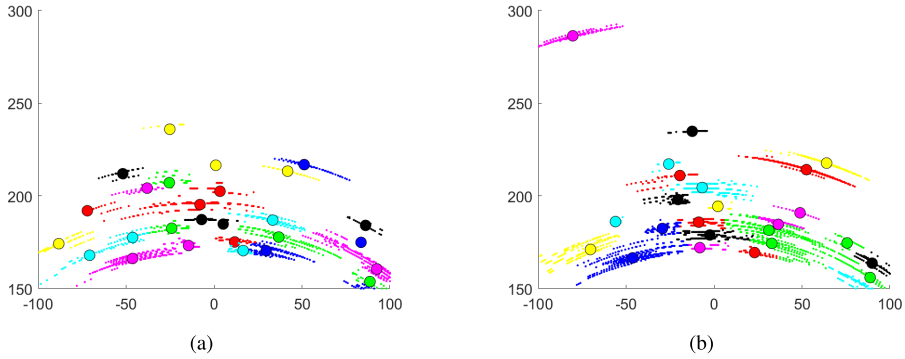

FIGURE 6. Meanshift cluster: (a) bearing-range spectrum 260; (b) bearing-range spectrum 271.

setting should be adjusted according to the two dimensions' resolution, time delay, and Doppler.

The measurement sets are shown in Fig. 7. The threshold of left and right sub-arrays can only be reduced to meet the same detection probability, so the total number of measurements in the left and right sub-arrays measurement set is more than that of the MIMO measurement set. More clutter in the measurement set also confirms that MIMO uses space diversity to reduce missing detection probability under the same false alarm probability. After obtaining the measurement set, Bernoulli filter is used to track the target. The surveillance area is a sector. The angle range is from $-45°$ to $45°$ and the distance range is from 150m to 350m. The total observation frames are 51 from 250 to 300. The probability of target survival and detection are 0.99 and 0.90 respectively.

In model prediction step, the state transition matrix is set to be a uniform linear model as follows:

$$\mathrm{F} = \begin{bmatrix} 1 & 1 & 0 & 0 \\ 0 & 1 & 0 & 0 \\ 0 & 0 & 1 & 1 \\ 0 & 0 & 0 & 1 \end{bmatrix} \tag{43}$$

and the process noise $v \sim \mathcal{N}\left(0, \sigma_v^2 I\right)$ with $\sigma_v^2 = 1$. In state update step, the position information should be changed from Cartesian coordinate system to polar coordinate system, and the observation noise $w \sim \mathcal{N}\left(0, R\right)$ with $R = \mathrm{diag}\left(\left[\frac{\pi}{180}, 2\right]\right)$.

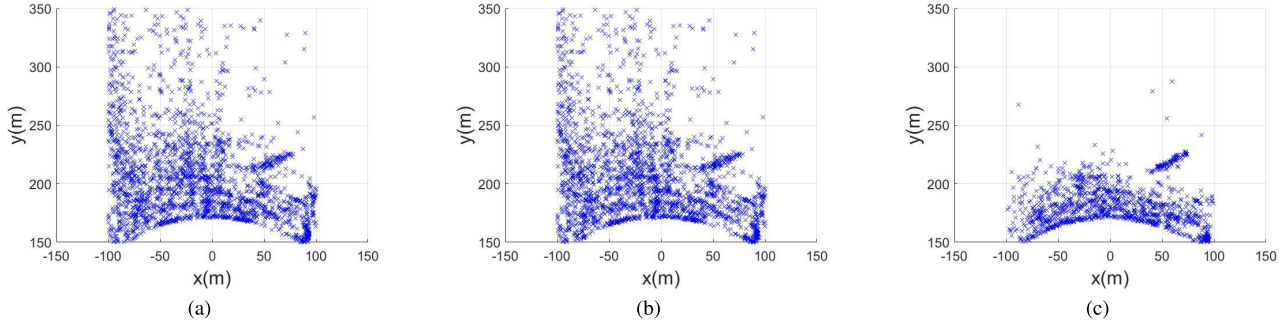

FIGURE 7. Measurement set: (a) Left sub-array; (b) Right sub-array; (c) MIMO.

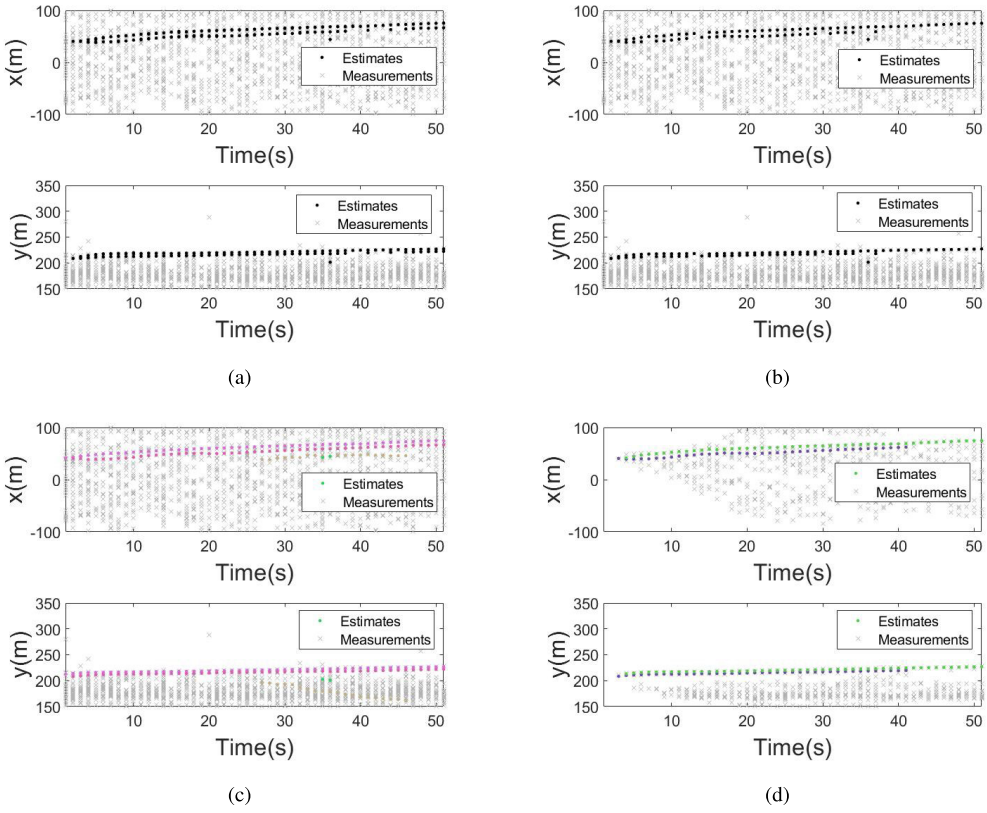

FIGURE 8. Bernoulli filter: (a) MEMBer filter; (b) CBMEMBer filter; (c) δ-GLMB filter; (d) δ-CBGLMB filter.

The birth process is a multi-Bernoulli RFS with probability $r = 0.02$ and variance $B = \text{diag}([3, 1, 3, 1])$. Four potential target positions are set in $[-40, 155]$, $[40, 205]$, $[-50, 255]$, $[50, 305]$ respectively and the initial speed of all potential targets are set to 0 m/s. In Fig. 8, the results of the MEMBer, CBMEMBer, δ-GLMB and δ-CBGLMB filters are showed. All the four filters use CKF in state update step.

In all the four filters, targets are tracked successfully. It proves the effectiveness of our distributed MIMO detection framework. Comparing the MEMBer with CBMEMBer filters in subfigure (a) and (b), it can be found that the MEMBer filter has a significant bias in the number of targets. In almost the entire tracking process, the MEMBer filter has four or five targets, and they are very close in the latter part of the subfigure (a). The CBMEMBer filter solves this problem very well, although there are still overestimation problems at some time. The correct target number and trajectories can still be clearly found. Comparing the CBMEMBer with δ-GLMB filters in subfigure (b) and (c), though the δ-GLMB filter can correctly identify each trajectory, it also has a specific terrain overestimation problem. Finally, the proposed δ-CBGLMB filter combines the advantages of the CBMEMBer and δ-GLMB filter, which not only reduces the problem of cardinality overestimation but also effectively

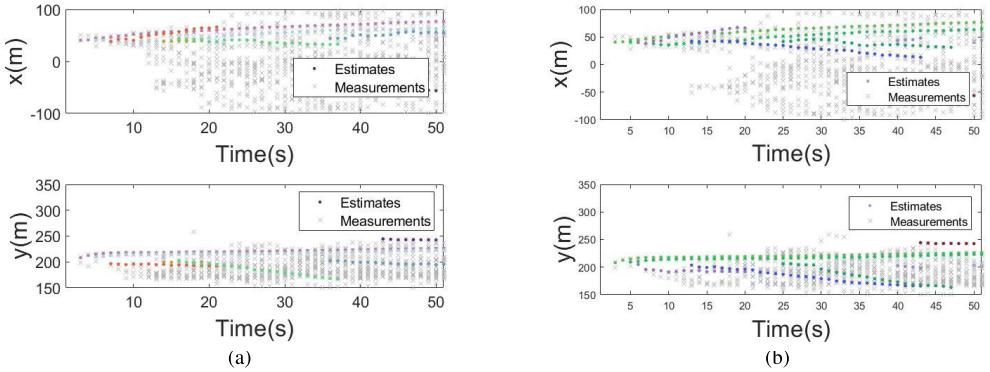

FIGURE 9. δ-CBGLMB filter: (a) Left sub-array; (b) Right sub-array.

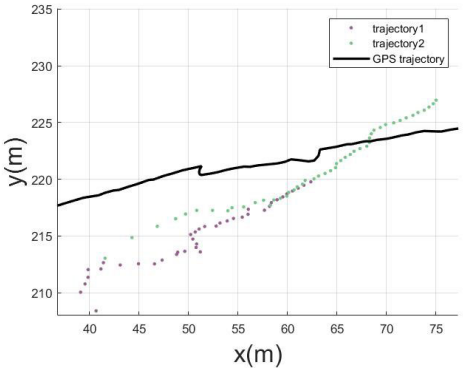

FIGURE 10. Trajectory.

identifies each trajectory, allowing us to judge the target motion more clearly. What is more, the δ-CBGLMB filter extracts a more accurate measurement set through the CBMEMBer filter and then performs δ-GLMB tracking, which effectively reduces the number of trajectory hypotheses in the label Bernoulli. Therefore, although the new filter's complexity is the same as the old filter, the efficiency of the algorithm has been improved.

To further evaluate the detection performance of distributed MIMO system, the tracking results of the left and right sub-arrays are shown in Fig. 9. Because the left and right sub-arrays are forced to lower the threshold during the clutter set extraction step in order to guarantee the same detection probability, multiple non-existent target trajectories are tracked, which also proves that the target tracking performance under the MIMO framework is far superior to that under the phased-array processing framework

Fig. 10 contains GPS target motion trajectory and two-dimensional δ-CBGLMB filter figure to verify further that our algorithm successfully tracks the targets. The deviation of the trajectory direction is produced by GPS positioning and Miller map.

VI. CONCLUSION

In this paper, a practical distributed MIMO detection framework was proposed for improving the ability to detect and track motion targets in shallow ocean environments. The distributed MIMO system outperformed the phased array system due to target diversity, which was supported by the sea experimental results. The RCI was combined with the δ-CBGLMB filter, which can stable track targets in a shallow ocean environment after a meanshift algorithm was carried out over the bearing-range spectrums. The improved Bernoulli filter had a smaller cardinality estimation bias than the δ-GLMB at low computation cost. Meanwhile, our filter can obtain the target trajectory label in comparison with the CBMEMBer filter.

APPENDIX

Based on the hypothsis that the noise received is IID, The conditional propobality density in $\mathcal{H}_1$ and $\mathcal{H}_0$ are

$$p_1\left(\mathbf{y} \mid \gamma_p, \mathbf{s}\right) = c_n \prod_{i=1}^{N_t} p_1^i\left(\mathbf{y}^i \mid \gamma_p^i, \mathbf{s}^i\right), \tag{44}$$

$$p_0(\mathbf{y}) = c_n \exp\left\{-\frac{1}{\sigma^2}\|\mathbf{y}\|^2\right\}, \tag{45}$$

where $c_n = \left(\pi\sigma^2\right)^{-N_t N_r L}$, $p_1^i\left(y^i \mid \gamma_p^i, s^i\right)$ can be written as follows:

$$p_1^i\left(\mathbf{y}^i \mid \gamma_p^i, \mathbf{s}^i\right) = \exp\left\{-\frac{1}{\sigma^2}\sum_{j=1}^{N_r}\left\|\mathbf{y}^{ij} - \gamma_p^{ij}\left(\mathbf{a}_p^{ij} \otimes D_p^{ij}\right)\mathbf{s}^i\right\|^2\right\}. \tag{46}$$

Because $\mathbf{s}$ and γ_p are unknown, they can be replaced by using maximum likelihood estimates (MLE), which is called GLRT. The definition of GLRT can be written:

$$\max_{\{\gamma_p, \mathbf{s}\}} l_1\left(\gamma_p, \mathbf{s} \mid \mathbf{y}\right) - l_0(\mathbf{y}) \underset{\mathcal{H}_1}{\overset{\mathcal{H}_1}{\gtrless}} \kappa, \tag{47}$$

where $l_1\left(\gamma_p, \mathbf{s} \mid \mathbf{y}\right) = \log p_1\left(\mathbf{y} \mid \gamma_p, \mathbf{s}\right)$, $l_0(\mathbf{y}) = \log p_0(\mathbf{y})$, κ is determined by false alarm rate (FAR). (46) is bring to (44) and ignore the constant. $l_1\left(\gamma_p, \mathbf{s} \mid \mathbf{y}\right)$ can be written as follows:

$$l_1\left(\gamma_p, \mathbf{s} \mid \mathbf{y}\right) = -\frac{1}{\sigma^2}\sum_{i=1}^{N_t}\sum_{j=1}^{N_r}\left\|\mathbf{y}^{ij} - \gamma_p^{ij}\left(\mathbf{a}_p^{ij} \otimes D_p^{ij}\right)\mathbf{s}^i\right\|^2. \tag{48}$$

Then the MLE of γ_p^{ij} is given by

$$\hat{\gamma}_p^{ij} = \frac{\left(\left(\mathbf{a}_p^{ij} \otimes D_p^{ij}\right)\mathbf{s}^i\right)^H \mathbf{y}^{ij}}{\left\|\left(\mathbf{a}_p^{ij} \otimes D_p^{ij}\right)\mathbf{s}^i\right\|^2} = \frac{\mathbf{s}^{iH}\tilde{\mathbf{y}}_b^{ij}}{\sqrt{N_e}\left\|\mathbf{s}^i\right\|^2}, \tag{49}$$

where $\tilde{\mathbf{y}}_b^{ij} = \left(D_p^{ij}\right)^H \mathbf{y}_b^{ij}$, $\mathbf{y}_b^{ij} = \frac{1}{\sqrt{N_e}}\sum_{n=1}^{N_r}\left[\mathbf{a}_p^{ij}\right]_n^* \mathbf{y}_n^{ij}$.

Bringing (49) back to (48)

$$l_1\left(\hat{\gamma}_p, \mathbf{s} \mid \mathbf{y}\right) = -\frac{1}{\sigma^2}\sum_{i=1}^{N_t}\left(\left\|\mathbf{y}^i\right\|^2 - \frac{\mathbf{s}^{iH}\Phi^i\Phi^i\mathbf{s}^i}{\left\|\mathbf{s}^i\right\|^2}\right), \tag{50}$$

where $\Phi^i = \left[\tilde{\mathbf{y}}_b^{i1}, \cdots, \tilde{\mathbf{y}}_b^{iN_r}\right]$.

Based on the rayleigh quotient (RQ) when $\mathbf{s} = \mathbf{v}_1\left(\Phi^i\Phi^{iH}\right)$, (50) reaches the maximum value. Bring $\mathbf{s} = \mathbf{v}_1\left(\Phi^i\Phi^{iH}\right)$ back to (50)

$$l_1\left(\hat{\gamma}_p, \hat{\mathbf{s}} \mid \mathbf{y}\right) = -\frac{1}{\sigma^2}\|\mathbf{s}\|^2 + \frac{1}{\sigma^2}\sum_{i=1}^{N_t}\lambda_1\left(\Phi^i\Phi^{iH}\right) \tag{51}$$

Similarly, under the assumption $\mathcal{H}_0$

$$l_0(\mathbf{y}) = -\frac{1}{\sigma^2}\|\mathbf{y}\|^2 \tag{52}$$

Combining (47), (51) and (52), the GLRT detector becomes

$$\sum_{i=1}^{N_t}\lambda_1\left(\Phi^i\Phi^{iH}\right) \underset{\mathcal{H}_1}{\overset{\mathcal{H}_1}{\gtrless}} \kappa. \tag{53}$$

REFERENCES

[1] X. Pan, S. Hui, X. Wen, and N. R. Chapman, "TR-MIMO detection of a small target in a shallow water waveguide environment," *Appl. Acoust.*, vol. 79, pp. 16–22, May 2014.

[2] X. Pan, Z. Ding, J. Jiang, and X. Gong, "Robust time-reversal is combined with distributed multiple-input multiple-output sonar for detection of small targets in shallow water environments," *Appl. Acoust.*, vol. 133, pp. 157–167, Apr. 2018.

[3] X. Pan, S. Li, and C. Pan, "Distributed broadband phased-MIMO sonar for detection of small targets in shallow water environments," *IET Radar, Sonar Navigat.*, vol. 12, no. 7, pp. 721–728, Jul. 2018.

[4] G. J. Foschini and M. J. Gans, "On limits of wireless communications in a fading environment when using multiple antennas," *Wireless Pers. Commun.*, vol. 6, no. 3, pp. 311–335, Mar. 1998.

[5] D. Gesbert, H. Bolcskei, D. A. Gore, and A. J. Paulraj, "Outdoor MIMO wireless channels: Models and performance prediction," *IEEE Trans. Commun.*, vol. 50, no. 12, pp. 1926–1934, Dec. 2002.

[6] E. Fishler, A. Haimovich, R. Blum, D. Chizhik, L. Cimini, and R. Valenzuela, "MIMO radar: An idea whose time has come," in *Proc. IEEE Radar Conf.*, Apr. 2004, pp. 71–78.

[7] J. Li and P. Stoica, "MIMO radar with colocated antennas," *IEEE Signal Process. Mag.*, vol. 24, no. 5, pp. 106–114, Sep. 2007.

[8] J. Liu, S. Zhou, W. Liu, J. Zheng, H. Liu, and J. Li, "Tunable adaptive detection in colocated MIMO radar," *IEEE Trans. Signal Process.*, vol. 66, no. 4, pp. 1080–1092, Feb. 2018.

[9] D. E. Hack, L. K. Patton, B. Himed, and M. A. Saville, "Centralized passive MIMO radar detection without direct-path reference signals," *IEEE Trans. Signal Process.*, vol. 62, no. 11, pp. 3013–3023, Jun. 2014.

[10] A. M. Haimovich, R. S. Blum, and L. J. Cimini, "MIMO radar with widely separated antennas," *IEEE Signal Process. Mag.*, vol. 25, no. 1, pp. 116–129, Jan. 2008.

[11] H. Li, Z. Wang, J. Liu, and B. Himed, "Moving target detection in distributed MIMO radar on moving platforms," *IEEE J. Sel. Topics Signal Process.*, vol. 9, no. 8, pp. 1524–1535, Dec. 2015.

[12] I. Bekkerman and J. Tabrikian, "Target detection and localization using MIMO radars and sonars," *IEEE Trans. Signal Process.*, vol. 54, no. 10, pp. 3873–3883, Oct. 2006.

[13] W. Li, G. Chen, E. Blasch, and R. Lynch, "Cognitive MIMO sonar based robust target detection for harbor and maritime surveillance applications," in *Proc. IEEE Aerosp. Conf.*, Mar. 2009, pp. 1–9.

[14] R. van Vossen, L. te Raa, and G. Blacquière, "Acquisition concepts for MIMO sonar," *Underwater Acoustic Measurments Proc.*, to be published. [Online]. Available: https://www.researchgate.net/publication/229046330_ACQUISITION_CONCEPTS_FOR_MIMO_SONAR

[15] Y. Pailhas, Y. Petillot, K. Brown, and B. Mulgrew, "Spatially distributed MIMO sonar systems: Principles and capabilities," *IEEE J. Ocean. Eng.*, vol. 42, no. 3, pp. 738–751, Jul. 2017.

[16] R. E. Kalman, "A new approach to linear filtering and prediction problems," *Trans. ASME, D, J. Basic Eng.*, vol. 82, no. 1, pp. 35–45, 1960.

[17] I. Arasaratnam and S. Haykin, "Cubature Kalman filters," *IEEE Trans. Autom. Control*, vol. 54, no. 6, pp. 1254–1269, Jun. 2009.

[18] X. Pan, Y. Bao, Y. Zhu, H. Dai, and J. Zhang, "Deconvolved conventional beamforming and adaptive cubature Kalman filter based distant speech perception system," *IEEE Access*, vol. 8, pp. 187948–187958, 2020.

[19] R. P. S. Mahler, "The Random-set approach to data fusion," *Proc. SPIE*, vol. 2234, pp. 287–295, Jul. 1994.

[20] R. P. S. Mahler, "Multitarget Bayes filtering via first-order multitarget moments," *IEEE Trans. Aerosp. Electron. Syst.*, vol. 39, no. 4, pp. 1152–1178, Oct. 2003.

[21] R. Mahler, "PHD filters of higher order in target number," *IEEE Trans. Aerosp. Electron. Syst.*, vol. 43, no. 4, pp. 1523–1543, Oct. 2007.

[22] R. P. S. Mahler, *Statistical Multisource-Multitarget Information Fusion*. Norwood, MA, USA: Artech House, 2007.

[23] B.-T. Vo, B.-N. Vo, and A. Cantoni, "The cardinality balanced multi-target multi-Bernoulli filter and its implementations," *IEEE Trans. Signal Process.*, vol. 57, no. 2, pp. 409–423, Feb. 2009.

[24] B.-T. Vo and B.-N. Vo, "Labeled random finite sets and multi-object conjugate priors," *IEEE Trans. Signal Process.*, vol. 61, no. 13, pp. 3460–3475, Jul. 2013.

[25] B. N. Vo, B. T. Vo, and D. Phung, "Labeled random finite sets and the Bayes multi-target tracking filter," *IEEE Trans. Signal Process.*, vol. 62, no. 24, pp. 6554–6567, Dec. 2014.

[26] B.-T. Vo, B.-N. Vo, and H. G. Hoang, "An efficient implementation of the generalized labeled multi-Bernoulli filter," *IEEE Trans. Signal Process.*, vol. 65, no. 8, pp. 1975–1987, Apr. 2017.

[27] Y. Yu, "Distributed multimodel Bernoulli filters for maneuvering target tracking," *IEEE Sensors J.*, vol. 18, no. 14, pp. 5885–5896, Jul. 2018.

[28] X. Shen, Z. Song, H. Fan, and Q. Fu, "General Bernoulli filter for arbitrary clutter and target measurement processes," *IEEE Signal Process. Lett.*, vol. 25, no. 10, pp. 1525–1529, Oct. 2018.

[29] W. J. Park and C. G. Park, "Multi-target tracking based on Gaussian mixture labeled multi-Bernoulli filter with adaptive gating," in *Proc. 1st Int. Symp. Instrum., Control, Artif. Intell., Robot. (ICA-SYMP)*, Jan. 2019, pp. 226–229.

[30] H. Tao, X. Shen, and Q. Deng, "Infrared target tracking algorithm based on Bernoulli filter and support vector machine," in *Proc. Int. Conf. Inf. Sci. Educ. (ICISE-IE)*, Dec. 2020, pp. 277–281.

[31] K. Shen, P. Dong, Z. Jing, and H. Leung, "Consensus-based labeled multi-Bernoulli filter for multitarget tracking in distributed sensor network," *IEEE Trans. Cybern.*, early access, Jul. 8, 2021, doi: 10.1109/TCYB.2021.3087521.

[32] B. Friedlander and A. Zeira, "Detection of broadband signals in frequency and time dispersive channels," *IEEE Trans. Signal Process.*, vol. 44, no. 7, pp. 1613–1622, Jul. 1996.

[33] T. Cacoullos, "Estimation of a multivariate density," *Ann. Inst. Statist. Math.*, vol. 18, no. 1, pp. 179–189, Dec. 1966.

[34] K. Fukunaga and L. Hostetler, "The estimation of the gradient of a density function, with applications in pattern recognition," *IEEE Trans. Inf. Theory*, vol. IT-21, no. 1, pp. 32–40, Jan. 1975.

[35] J. Berclaz, F. Fleuret, E. Türetken, and P. Fua, "Multiple object tracking using k-shortest paths optimization," *IEEE Trans. Pattern Anal. Mach. Intell.*, vol. 33, no. 9, pp. 1806–1819, Sep. 2011.

[36] R. Bellman, "On a routing problem," *Quart. Appl. Math.*, vol. 16, no. 1, pp. 87–90, 1958.

[37] K. G. Murty, "An algorithm for ranking all the assignments in order of increasing cost," *Oper. Res.*, vol. 16, pp. 682–687, May/Jun. 1968.

HUANGYU DAI received the B.Eng. degree in electronic information science and technology from Dalian Maritime University, Dalian, China, in 2019. He is currently pursuing the D.Eng. degree in information and communication engineering with Zhejiang University, Hangzhou, China.

XIANG PAN received the bachelor's degree in underwater acoustic electronic engineering from Harbin Ship Engineering Institute, in 1989, the master's degree in underwater acoustic engineering from China Ship Research and Development Academy, in 1998, and the Ph.D. degree in information and communication engineering from Zhejiang University, in 2003.

He is currently an Associate Professor with Zhejiang University. He was a Visiting Scholar with Concordia University, Canada, from June 2009 to September 2009; the University of Victoria, Canada, from April 2011 to April 2012; and the University of Connecticut, USA, from May 2014 to September 2014. His research interests include areas of statistical signal processing, acoustic signal processing, pattern recognition, and image processing.

ZHONGDI LIU received the B.Eng. degree in electronic information and communications from Huazhong University of Science and Technology, Wuhan, China, in 2019. She is currently pursuing the M.Eng. degree in information and communication engineering with Zhejiang University, Hangzhou, China.

PENG ZHANG received the B.Eng. degree in information and communication engineering from Hohai University, Nanjing, China, in 2019. He is currently pursuing the M.Eng. degree in information and communication engineering with Zhejiang University, Hangzhou, China.

ZHONGYONG CHEN received the Graduate degree from the Department of Biomedical Engineering and Instruments, Zhejiang University. He is currently working with the Information Center, Zhejiang Drug Administration Bureau, mainly engaged in the research and development of information management system of drugs and medical devices, risk analysis, and risk control.